

Single production of vectorlike quarks with charge 5/3 at the 14 TeV LHC

Yao-Bei Liu*, Bo Hu, Chao-Zheng Li

Henan Institute of Science and Technology, Xinxiang 453003, P.R. China

Abstract

In a framework of the Standard Model (SM) simply extended by an SU(2) doublet (X, T) including a vectorlike X -quark (VLQ- X), with electric charge $|Q_X| = 5/3$, we investigate the single production of the VLQ- X induced by the couplings between the VLQ- X with the first and the third generation quarks at the Large Hadron Collider (LHC) operating at $\sqrt{s} = 14$ TeV. The signal is searched in events including same-sign dileptons (electrons or muons), one b -tagged jet and missing energy, where the X quark is assumed to decay into a top quark and a W boson, both decaying leptonically. After a rapid simulation of signal and background events, the 95% CL exclusion limits and the 5σ discovery reach are respectively obtained at the LHC with an integrated luminosity of 300 and 3000 fb $^{-1}$, respectively.

arXiv:2402.01248v4 [hep-ph] 4 Sep 2024

* E-mail: liuyaobei@hist.edu.cn

I. INTRODUCTION

To promote a potential solution to the gauge hierarchy problem [1], new vectorlike quarks (VLQs) with mass at the TeV scale are often present in many extensions of the Standard Model (SM), such as little Higgs models [2–5], composite Higgs models [6–9], and other extended models [10–13], in which they cancel top-quark loop contributions to the Higgs mass [14]. In the renormalizable extensions of the SM, the canonical representation of VLQs generally constitutes one of seven multiplets VLQs, including two singlet $[T, B]$, three doublets $[(X, T), (T, B)$ or $(B, Y)]$, and two triplets $[(X, T, B)$ or $(T, B, Y)]$. In the proposed model, T and B can be regarded as the top and bottom partners, respectively. Y and X quarks have exotic electric charges of $-4/3$ and $5/3$, respectively. Here we concentrate on the vectorlike X -quark (VLQ- X), which commonly occurs as part of an $SU(2)_L \times SU(2)_R$ bi-doublet in models that preserve the custodial symmetry [15, 16], and in models where some VLQs are added via renormalizable couplings [17, 18]. Furthermore, such new particles could generate characteristic signatures at the Large Hadron Collider (LHC) and future high-energy colliders (see, for example [19–49]).

The ATLAS and CMS collaborations have conducted extensive searches for the pair production of VLQ- X [50–56]. In the absence of any discovery, these searches have put strong limits on VLQs masses according to the assumed decay pattern. For instance, CMS Collaboration used an integrated luminosity 35.9 fb^{-1} of data and provided the lower mass bounds about 1.30 (1.33) TeV at 95% confidence level (C.L.), for the case of left (right)-handed couplings to W bosons in a combination of the same-sign dileptons and single-lepton final states [57]. Recently, the search was carried out on 139 fb^{-1} of proton-proton collision data at $\sqrt{s} = 13 \text{ TeV}$ with the ATLAS detector between 2015 and 2018 runs [58]. This search excluded the presence of a VLQ- X with mass up to 1.46 TeV for (X, T) doublets for $Br(X \rightarrow tW) = 1$. Besides, such VLQ- X can also be singly produced at the LHC via its electroweak (EW) coupling, which is model-dependent and always depends on the EW coupling strength [59–61]. Considering the final state including one muon or electron, the VLQ- X with a relative width of 10%, 20%, and 30% of its mass can be excluded below 0.92, 1.3, and 1.45 TeV, respectively at the $\sqrt{s} = 13 \text{ TeV}$ LHC by the CMS Collaboration [62].

The upgrade of the LHC to the high-luminosity phase (HL-LHC) [63] at center-of-mass energy of 14 TeV with an integrated luminosity of 3000 fb^{-1} will extend the sensitivity and per-

spectives to discover possible new physics signals. Due to the exotic charge, its main distinctive decay mode is $X \rightarrow t(\rightarrow W^+b)W^+$, which can give rise to the final states including same-sign two leptons (SS2L) via the W leptonic decays. In comparison with the existing searches for other channels, the SS2L channel has the great advantage that most QCD backgrounds are gone, such as done in Refs. [64–71]. Considering VLQ- X pair production and looking for a SS2L channel, the bounds on the VLQ- X mass obtained from ATLAS (CMS) are $M_X > 670$ (675) GeV with a sample corresponding to an integrated luminosity of 4.7 (5) fb^{-1} [72, 73].

Although the new VLQs are typically considered to mix sizably only with the third-generation of SM quarks, partial mixing to the first two generation SM quarks is not completely excluded [17]. This is because cancellations among the effects of different types of new VLQs can significantly alleviate the indirect constraints [74–82]. Especially, the EW precision bounds on the extra VLQs are generally weaker than the corresponding bounds on the extra chiral quarks such as the fourth family quarks/leptons [83]. The crucial point is that even a small mixing to the first generation may have a severe impact on single VLQs production processes due to the presence of valence quarks in the initial state at the LHC [84–86]. Very recently, the ATLAS Collaboration used an integrated luminosity 140 fb^{-1} of data and excludes VLQs with masses below 1530 GeV for the branching ratio $Br(Q \rightarrow Wq) = 1$ [87]. In this work, we study the single production of the VLQ- X at the HL-LHC in a simplified scenario where the VLQ- X could mix with both the first-generation and the third-generation SM quarks, as shown in Fig. 1, and then analyze the SS2L final state via $X \rightarrow t(\rightarrow bW^+)W^+$ decay channel followed by the W leptonic decays mode. Consequently, this analysis complements the more common searches for VLQ- X that are assumed to mix only with the third-generation SM quarks [88, 89].

The paper is arranged as follows. In Sec. II, we consider an effective model framework including the VLQ- X and calculate its single production cross sections at the 14 TeV LHC involving the mixing with both the first and third generate quarks. In Sec. III, we discuss its observability via the decay mode $X \rightarrow t(\rightarrow bW^+)W^+ \rightarrow \ell^+\ell^+b + \cancel{E}_T$ at the HL-LHC. Finally, conclusions are presented in Sec. IV.

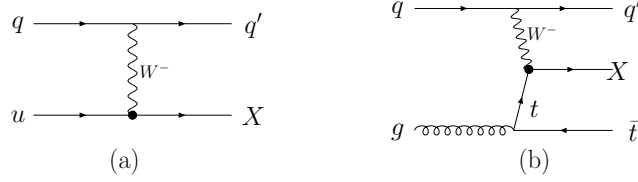


FIG. 1: Representative Feynman diagrams for the single production processes at the LHC via couplings of the X to (a) first generation quarks and (b) third generation quarks.

II. VLQ- X IN A SIMPLIFIED MODEL

A. An effective Lagrangian for doublet VLQ- X

In general, the new fermions are assumed to interact with the SM fermions via Yukawa interactions, whose quantum numbers with respect to the weak $SU(2)_L \times U(1)_Y$ gauge group are thus limited by the requirement of an interaction with the Higgs doublet and one of the SM fermions (see for example [23] and references therein). Here we focus on a specific simple model containing a vectorlike quark which is an $SU(2)$ doublet with the hypercharge $7/6$. It is worth mentioning that such a new doublet also contains a vectorlike T -quark with electric charge of $2/3$ due to its mixing with SM up-type quarks. The Yukawa couplings induced by the new doublet $(X, U)^T$ generate a mixing in the up sector, with the three lighter mass eigenstates identified with the SM quarks. Assuming that u_R^i and u_L^i represent the SM singlets and up component of the doublets, the mass terms are given by [24],

$$\mathcal{L}_{\text{mass}} = - \sum_{i=1}^3 \frac{y_u^i v}{\sqrt{2}} \bar{u}_L^i u_R^i - \sum_{i=1}^3 x_i \bar{U}_L u_R^i - M \bar{U}_L U_R - M \bar{X}_L X_R + h.c., \quad (1)$$

where y_u^i are the diagonal SM up Yukawa interactions, $v \sim 246$ GeV is the Higgs vacuum expectation value (VEV), $x_i = \frac{\lambda^i v}{\sqrt{2}}$ represents the mixing generated by the Higgs VEV and λ^i denote the new Yukawa couplings connecting the heavy quarks with the SM ones, M is the vector-like quark mass.

We have not explicitly written down the heavy quark Higgs couplings because they do not contribute appreciably to the production process of our interest, and the details of the mixing

matrices including all three families of quarks in the SM can be found in Refs. [23, 24]. As shown in Ref. [24], the couplings of VLQ- X with the up-type SM quarks are generated by the coupling with its $SU(2)$ partner U , which mixes with the SM up quarks. The W -boson interactions with the SM quarks and VLQ- X are given by:

$$\begin{aligned} \mathcal{L}_X = & i\frac{g}{\sqrt{2}} W_\mu^+ \bar{X}_R \gamma^\mu (V_R^{43} t_R + V_R^{42} c_R + V_R^{41} u_R) + \\ & i\frac{g}{\sqrt{2}} W_\mu^+ \bar{X}_L \gamma^\mu (V_L^{43} t_L + V_L^{42} c_L + V_L^{41} u_L) + h.c., \end{aligned} \quad (2)$$

Here we have neglected terms proportional to the vectorlike T -quark and the remaining terms can be found in [23]. The matrix elements related to the new Yukawa couplings are given by

$$\begin{aligned} V_R^{41} = -\frac{x_1}{M}, \quad V_R^{42} = -\frac{x_2}{M}, \quad V_R^{43} = -\sin \theta_R; \\ V_L^{41} = -\frac{M_u x_1}{M^2}, \quad V_L^{42} = -\frac{M_c x_2}{M^2}, \quad V_L^{43} = -\frac{M_t}{M} \sin \theta_R. \end{aligned} \quad (3)$$

The above formulas show that the left-handed mixing with the light quarks, V_L^{41} and V_L^{42} , can be safely neglected being suppressed by the light quark masses (M_u and M_c), while the right-handed ones are proportional to the Yukawa masses x_i . Here we only simply recall the case for the VLQ- X which is relevant for our discussion. Therefore, our study primarily concentrates on the right-handed coupling part of the interactions involving the VLQ- X . Note that the matrices V_L and V_R will introduce a flavour mixing in the up sector, which can be strongly constrained by the flavor physics and the oblique parameters [90–93]. The stringent bound on flavour violation for this non-standard doublet case come from D_0 - \bar{D}_0 mixing: $|V_R^{41}||V_R^{42}| < 3.2 \times 10^{-4}$ [23]. However, the bounds on the individual mixing terms, V_R^{41} and V_R^{42} , are rather mild, i.e. $|V_R^{41}| < 7.8 \times 10^{-2}$ [23], which is obtained by Atomic Parity Violation (APV) experiments for the up, and $|V_R^{42}| < 0.2$, which come from the measurement of R_c at LEP [23].

In our simplified model, we assume that the VLQ- X couples only to the first- and third-generation quarks. An effective Lagrangian framework for the interactions of a VLQ- X with the SM quarks through the gauge boson W exchange is given by ¹

$$\mathcal{L}_X = g^* \left\{ \sqrt{\frac{R_L}{1+R_L}} \frac{g}{\sqrt{2}} [\bar{X}_R W_\mu^+ \gamma^\mu u_R] + \sqrt{\frac{1}{1+R_L}} \frac{g}{\sqrt{2}} [\bar{X}_R W_\mu^+ \gamma^\mu t_R] \right\} + h.c., \quad (4)$$

where g is the $SU(2)_L$ gauge coupling constant, g^* denotes the VLQ- X coupling strength to SM quarks in units of standard couplings, R_L is the generation mixing coupling and two factors

¹ Details are provided on the URL feynrules.irmp.ucl.ac.be/wiki/VLQ_xtdoubletvl.

$\frac{R_L}{1+R_L}$ and $\frac{1}{1+R_L}$ describe the decay rate of the VLQ- X to the first and third generation quark, respectively. In the extreme case, $R_L \rightarrow 0$ and $R_L \rightarrow \infty$, respectively, correspond to coupling to third-generation quarks and first-generation of quarks only.

Note that there are different symbols for the coupling coefficient in some literature [88–90], such as $\sin \theta_R$, κ and g^* . The relationship between these symbols of the coupling coefficient can be deduced as $\sin \theta_R = \kappa = g^*$ when $R_L = 0$ in this work. Assuming that the VLQs mix only with the third-generation quarks, the recent bound on the coupling parameter comes from the oblique parameters S , T and U : the precise bound is mass dependent, i.e., $\sin \theta_R < 0.42$ (0.25) for $M_X = 1.3$ (2.5) TeV in the (X, T) doublet model [90]. The strong limit for the up quark mixing come from the APV experiments: $|V_R^{41}| = g^* \sqrt{\frac{R_L}{1+R_L}} < 7.8 \times 10^{-2}$ [23]. For a typical value $g^* = 0.1$ (0.2), one can get $R_L < 1.55$ (0.18). Here we take only a phenomenologically guided limit and choose a slightly looser range: $g^* \leq 0.5$ and $0 \leq R_L \leq 1$.

B. Decay and production cross section

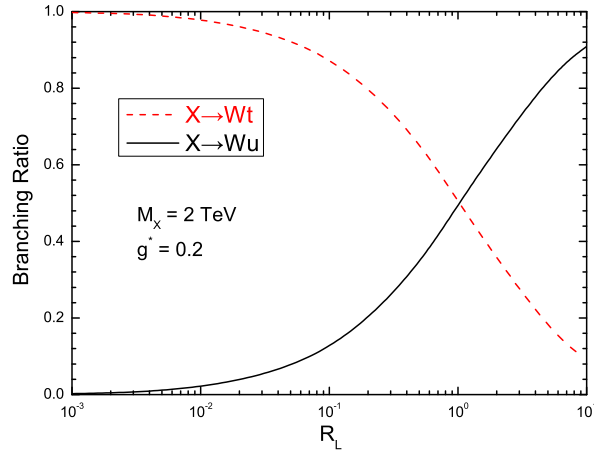


FIG. 2: The branching ratio as a function of R_L for $g^* = 0.2$ and $M_X = 2.0$ TeV.

Due to its charge, the VLQ- X can decay only to Wt and Wu therefore $BR(X \rightarrow Wt) + BR(X \rightarrow Wu) = 100\%$, as shown in Fig. 2. Note that, when R_L up to 1.0, the decay rate of VLQ- X to the first-generation quark reaches to the same value of VLQ- X to the third-

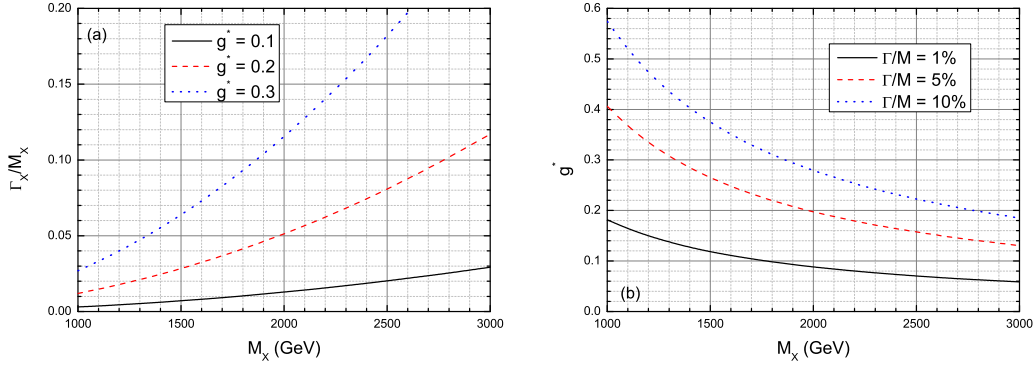


FIG. 3: (a) The width-over-mass ratio Γ_X/M_X as a function of M_X for three typical coupling strength $g^* = 0.1, 0.2$ and 0.3 . (b) The value of g^* as a function of M_X for different width-over-mass ratio $\Gamma_X/M_X = 1\%, 5\%$ and 10% .

generation quark decay. The decay width depends on the coupling parameter g^* and its mass M_X . For a fixed mass of VLQ- X , the total width Γ_X is always proportional to $(g^*)^2$, as shown in Fig. 3(a). Therefore, the coupling strength g^* can also be fixed to obtain a specific width-over-mass ratio Γ_X/M_X , as shown in Fig. 3(b). One can see that, for the scenario $\Gamma_X/M_X = 10\%$, g^* is approximately smaller than 0.2 in the whole range of explored masses. It has been pointed out in [94] that the Breit-Wigner (BW) form of a propagator may be appropriate for narrow resonances where the width-over-mass ratio is smaller than 10%. Thus the VLQ- X can be assumed with narrow decay widths and the production and decay can be factorised under the narrow-width approximation (NWA) case ².

The VLQ- X can be both single and pair produced at the LHC. The cross sections of single VLQ- X production versus its mass at the 14 TeV LHC has been presented in Fig. 4(a) with different coupling parameters. The leading-order (LO) cross sections are obtained using MadGraph5-aMC@NLO [95] with default NN23L01 parton distribution function (PDFs) [96] taking the default renormalization and factorization scales. One can note that pair production is only dominant at low masses of the VLQ- X but decreases faster than single production when the mass of the VLQ- X increases. This is due to the phase space suppression and the decrease

² See Refs. [59–61] for large-width effects in vector-like quark production.

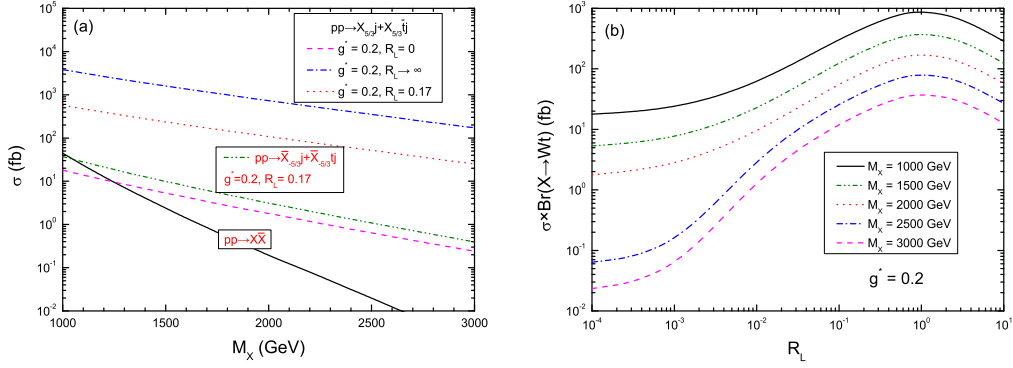


FIG. 4: (a) Cross sections of VLQ- X as a function of the mass M_X for single and pair production processes at the 14 TeV LHC. (b) Production cross section of $\sigma \times Br(X \rightarrow tW)$ as a function of R_L for $g^* = 0.2$ and five typical values of M_X at the 14 TeV LHC.

of the parton distribution functions with the centre of mass energy of the parton-level collision. However, single heavy quark production has the advantage of less phase-space suppression and longitudinal gauge boson enhancement of order M_X^2/M_W^2 at higher energies compared to pair production. With the fixed parameters $g^* = 0.2$ and $R_L = 0.17$, the cross section can reach about 236 (108) fb for $M_X = 1.5$ (2.0) TeV. We also plot the cross section for the process $pp \rightarrow \bar{X}j + \bar{X}tj$ for the same fixed coupling parameters. One can see that the production cross section of $pp \rightarrow Xj + X\bar{t}j$ is much larger than that for the conjugate process due to the difference in the PDFs of valence and sea quarks in the initial states.

In Fig. 4(b), we also show the dependence of the cross sections $\sigma \times Br(X \rightarrow tW)$ on the mixing parameter R_L . We generate five benchmark points varying the VLQ- X mass in steps of 500 GeV in the range [1000; 3000] GeV with $g^* = 0.2$. One can see that (i) in the range of $R_L < 1$, the production cross section increases largely with the increase of R_L . (ii) For $R_L > 1$, the production cross section will become small with the increase of R_L . This effect is mainly due to the increased admixture of valence quarks in production, mitigated by a reduced $X \rightarrow tW$ branching ratio with increasing R_L . The cross section will reach a maximum for $R_L \simeq 1$, which corresponds to 50% – 50% mixing.

III. EVENT GENERATION AND DISCOVERY POTENTIALITY

In this section, we analyze the 14 TeV LHC observation potential by performing a Monte Carlo simulation of the signal and SM background events and explore the sensitivity to the VLQ- X through the process

$$\begin{aligned}
 pp \rightarrow X(\rightarrow tW^+)j &\rightarrow t(\rightarrow bW^+ \rightarrow b\ell^+\nu_\ell)W^+(\rightarrow \ell^+\nu_\ell)j, \\
 pp \rightarrow X(\rightarrow tW^+)\bar{t}j &\rightarrow t(\rightarrow bW^+ \rightarrow b\ell^+\nu_\ell)W^+(\rightarrow \ell^+\nu_\ell)\bar{t}j,
 \end{aligned}
 \tag{5}$$

where $\ell = e, \mu$.

In this analysis, the final states with SSL (muon or electron), one b -tagged jet, and missing transverse energy \cancel{E}_T are studied. Note that we do not consider the reconstruction or selection for the associated anti-top quark as well as the leptons or jets originating from its decay, due to their much lower transverse momenta p_T . The dominant SM backgrounds come from the SM processes $t\bar{t}W^+$, W^+W^+ +jets and the nonprompt leptons (mainly from events with jets of heavy flavor, such as $t\bar{t}$). To account for contributions from higher-order QCD corrections, the cross sections of dominant backgrounds at LO are adjusted to NLO or next-NLO (NNLO) order using K -factors, which are listed in table I.

TABLE I: K -factors of the leading SM background processes for our analysis.

Process	W^+W^+jj	$t\bar{t}W^+$	$t\bar{t}$
K -factor	1.04 [97, 98]	1.22 [99]	1.6 [100]

Signal and background events are generated at LO using MadGraph5-aMC@NLO. To perform the parton shower and fast detector simulations, we transmit the parton-level events to Pythia8 [101] for parton showering and hadronization, then processed through Delphes 3.4.2 [102] for detector simulation by using the standard HL-LHC detector parameterization shipped with the program. Finally, the resulting signal and background events are analyzed using MadAnalysis5 [103].

To identify objects, the following basic cuts are chosen at parton level:

$$p_T^{\ell/j} > 30 \text{ GeV}, \quad |\eta_\ell| < 2.5, \quad |\eta_j| < 5, \quad \Delta R_{ij} > 0.4,
 \tag{6}$$

where $\Delta R = \sqrt{\Delta\Phi^2 + \Delta\eta^2}$ is the separation in the rapidity-azimuth plane and $p_T^{\ell/j}$ and $|\eta_{\ell/j}|$ are the transverse momentum and pseudorapidity of the leptons and jets, respectively.

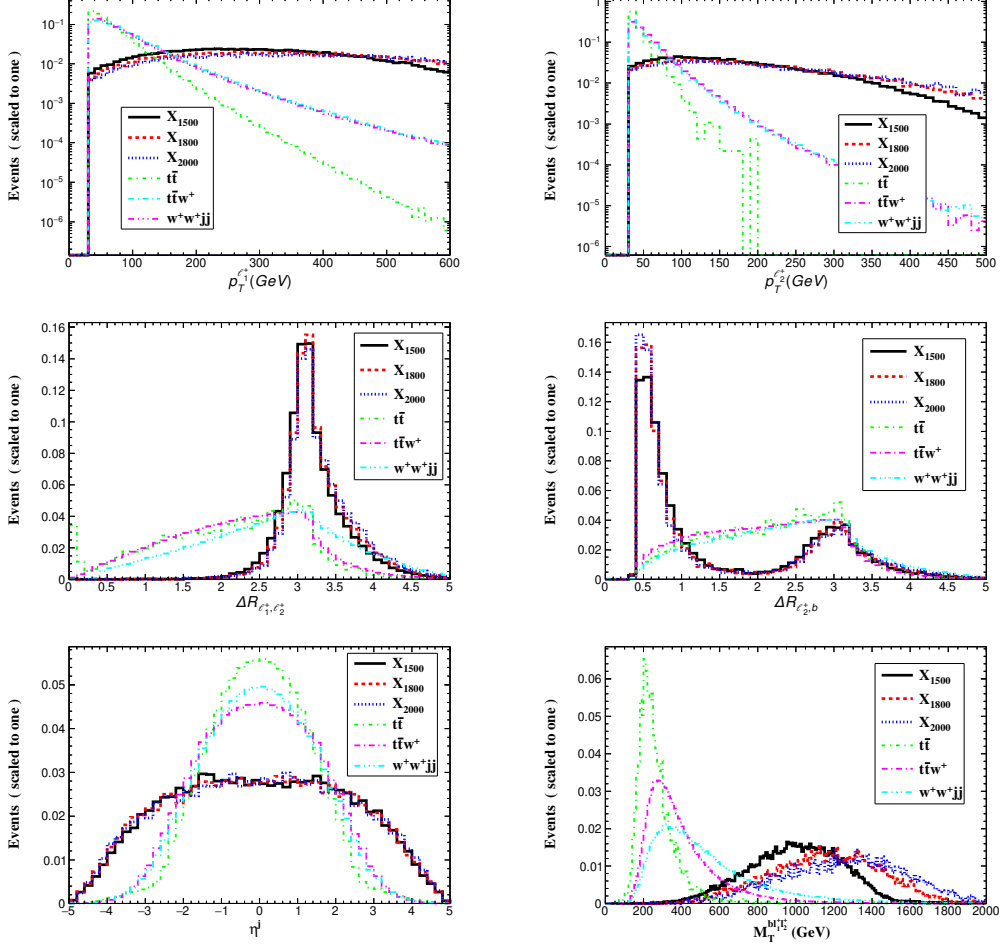


FIG. 5: Normalized distributions for the signals (with $M_X = 1500, 1800$ and 2000 GeV) and SM backgrounds.

In Fig. 5, we plot some differential distributions for signals and SM backgrounds at the LHC, such as the transverse momentum distributions of the leading and subleading leptons ($p_T^{\ell_{1,2}}$), the separations $\Delta R_{\ell_1, \ell_2}$ and $\Delta R_{\ell_2, b}$, the rapidity of the forward jet and the transverse mass³ distribution for VLQ- X $M_T^{bl\ell_2}$. Due to the larger mass of VLQ- X , the decay products are highly boosted, and thus the p_T^ℓ peaks of the signals are larger than those of the SM backgrounds.

³ The definition of the transverse mass of the system can be seen from Ref. [104].

Based on these kinematical distributions, we apply the following kinematic cuts to the events to distinguish the signal from the SM backgrounds.

- Cut 1: Exactly two same-sign isolated leptons [$N(\ell^+) = 2$] and the transverse momenta of the leading and subleading leptons are required $p_T^{\ell_{1,2}} > 120$ (60) GeV, the distance between two leptons lies in $\Delta R_{\ell_1, \ell_2} > 2.5$.
- Cut 2: At least one b -tagged jet [$N(b) \geq 1$] with $p_T^b > 30$ GeV. Besides, the distance between the subleading leptons with the b -tagged jet is required $\Delta R_{\ell_2, b} < 1$.
- Cut 3: Since the jet from splitting of a valence quark with one W emission always has a strong forward nature, the light untagged jet is required to have $|\eta_j| > 2$.
- Cut 4: The transverse mass of final system is required to have $M_T^{b\ell_1\ell_2} > 600$ GeV.

TABLE II: Cut flow of the cross sections (in fb) for the signals and SM backgrounds at the 14 TeV LHC and three typical VLQ- X masses. Here we set a benchmark value of $g^* = 0.2$ and $R_L = 0.17$.

Cuts	Signals			Backgrounds		
	1500 GeV	1800 GeV	2000 GeV	$t\bar{t}$	$t\bar{t}W^+$	W^+W^+jj
Basic	6.18	3.88	2.86	18741	11.1	2.73
Cut 1	2.44	1.38	0.94	0.1	0.32	0.11
Cut 2	0.78	0.44	0.28	0.01	0.06	8×10^{-4}
Cut 3	0.37	0.20	0.13	0.0022	0.009	1×10^{-4}
Cut 4	0.36	0.197	0.125	0.0011	0.0046	7.7×10^{-5}

In Table II, we present the cross sections of three typical signal ($M_X = 1500, 1800, 2000$ GeV) and the relevant backgrounds after imposing the above mentioned cuts. Notably, all background processes are suppressed very significantly at the end of the cut flow, and the dominant SM background comes from the $t\bar{t}W^+$ process, with a cross section of 4.6×10^{-3} fb.

The following statistical significance is used to estimate the expected discovery and exclu-

sion limits [105]

$$\begin{aligned}\mathcal{Z}_{\text{disc}} &= \sqrt{2 \left[(s+b) \ln \left(\frac{(s+b)(1+\delta^2 b)}{b+\delta^2 b(s+b)} \right) - \frac{1}{\delta^2} \ln \left(1 + \delta^2 \frac{s}{1+\delta^2 b} \right) \right]} \\ \mathcal{Z}_{\text{excl}} &= \sqrt{2 \left[s - b \ln \left(\frac{b+s+x}{2b} \right) - \frac{1}{\delta^2} \ln \left(\frac{b-s+x}{2b} \right) \right] - (b+s-x) \left(1 + \frac{1}{\delta^2 b} \right)},\end{aligned}\quad (7)$$

with

$$x = \sqrt{(s+b)^2 - 4\delta^2 s b^2 / (1 + \delta^2 b)}, \quad (8)$$

where s and b denote the event number of signal and background after the above cuts, respectively. The integrated luminosity at the 14 TeV LHC is set at 300 and 3000 fb^{-1} , respectively. δ denotes the percentage systematic uncertainty that inevitably appears in the measurement of the SM background. In the limit case ($\delta \rightarrow 0$), these expressions can be simplified as

$$\begin{aligned}\mathcal{Z}_{\text{disc}} &= \sqrt{2[(s+b) \ln(1+s/b) - s]}, \\ \mathcal{Z}_{\text{excl}} &= \sqrt{2[s - b \ln(1+s/b)]},\end{aligned}\quad (9)$$

as already used in many of the phenomenological studies.

In Fig. 6, we plot the excluded the 95% CL exclusion limit and 5σ discovery reaches in the plane of $g^* - M_X$ at the 14 TeV LHC with an integrated luminosity of 300 fb^{-1} and 3000 fb^{-1} respectively for three different systematic uncertainty cases: no systematics ($\delta = 0$), a mild systematic of $\delta = 10\%$, and a possible systematic of $\delta = 20\%$. One can see that with a possible uncertainty of 20%, sensitivities are slightly weaker than those with a mild systematic uncertainty of 10% and no systematics of $\delta = 0$. In the presence of 10% systematic uncertainty and $R_L = 0$, the discovered (with 5σ level) regions are $g^* \in [0.21, 0.4]$ ($[0.1, 0.4]$) and $M_X \in [1000, 1550]$ ($[1000, 2000]$) GeV at the 14 TeV LHC with an integrated luminosity of 300 (3000) fb^{-1} . Out of a discovery, the VLQ- X can be excluded (at 95% CL limits) in the correlated parameter space of $g^* \in [0.12, 0.4]$ ($[0.06, 0.4]$) and $M_X \in [1000, 1980]$ ($[1000, 2450]$) GeV for the same integrated luminosity. Assuming the non-vanishing R_L value, i.e., $R_L = 0.1$, the discovery region can reach $g^* \in [0.05, 0.39]$ ($[0.025, 0.2]$) and $M_X \in [1000, 3000]$ GeV with an integrated luminosity of 300 (3000) fb^{-1} . Otherwise, the 95% CL excluded region for the coupling parameter is $g^* \in [0.03, 0.21]$ ($[0.015, 0.11]$) and $M_X \in [1000, 3000]$ GeV with the same integrated luminosity at the 14 TeV LHC. Besides, although the vector like quark width plays a significant role in their single production, the region in this study is almost located in $\Gamma_X/M_X < 10\%$, and thus the NWA is reasonable in our study.

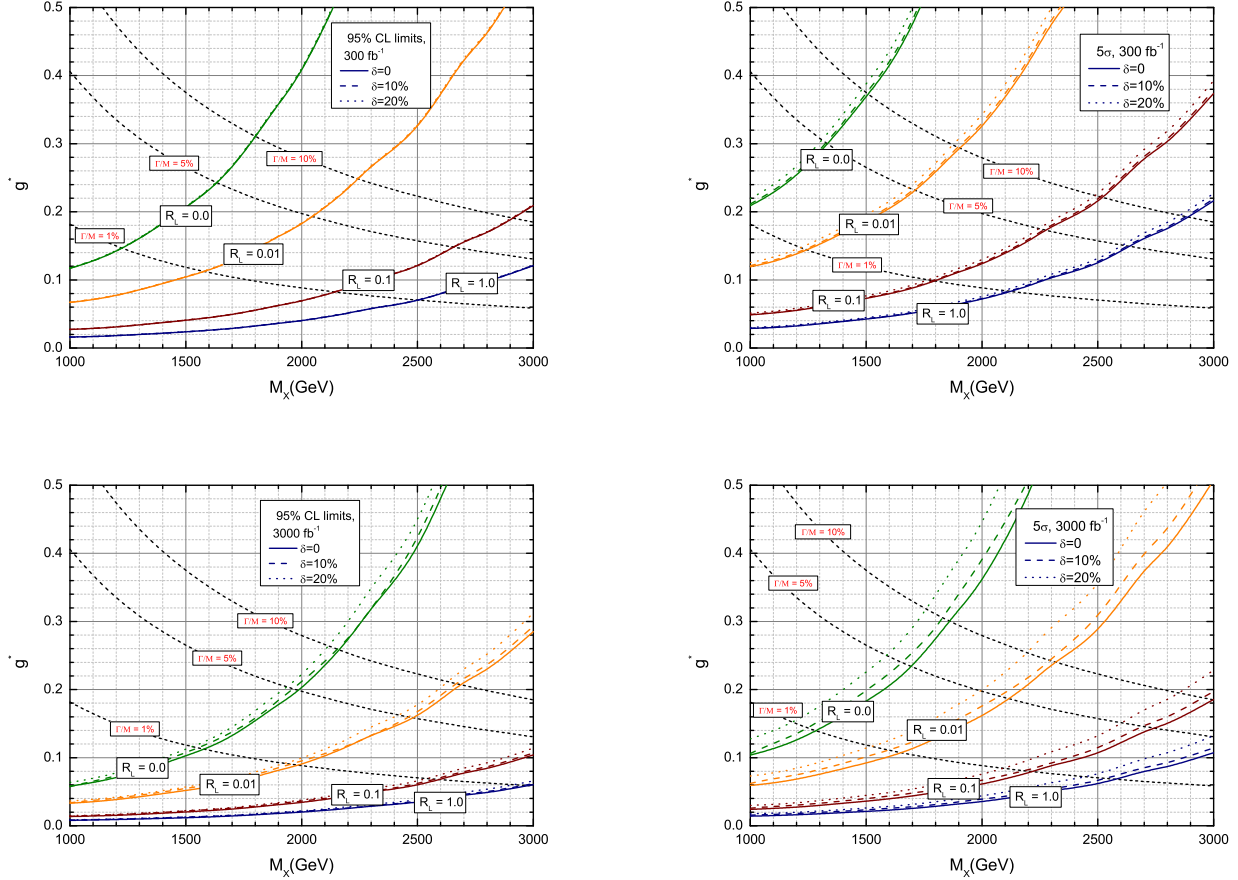


FIG. 6: 95% CL exclusion limit (left panel) and 5σ (right panel) contour plots for the signal in $g^* - M_X$ at the 14 TeV LHC with an integrated luminosity of 3000 fb^{-1} (upper) and 300 fb^{-1} (down). Short-dashed lines denote the contours of Γ_X/M_X .

The sensitivity that graphicized as contours in $g^* - R_L$ plane is presented in Fig. 7 with $\delta = 10\%$ and five fixed typical VLQ- X masses at the 14 TeV LHC with an integrated luminosity of 300 and 3000 fb^{-1} , respectively. The current limits from the APV experiment are also displayed as dot-dashed curves. One can see that, for $M_X = 1500, 2000, 2500 \text{ GeV}$ and $R_L = 0.1$, the 5σ level discovery sensitivity of g^* is respectively about 0.08, 0.14, 0.24 with an integrated luminosity of 300 fb^{-1} , and changed as about 0.05, 0.14, 0.13 with an integrated luminosity of

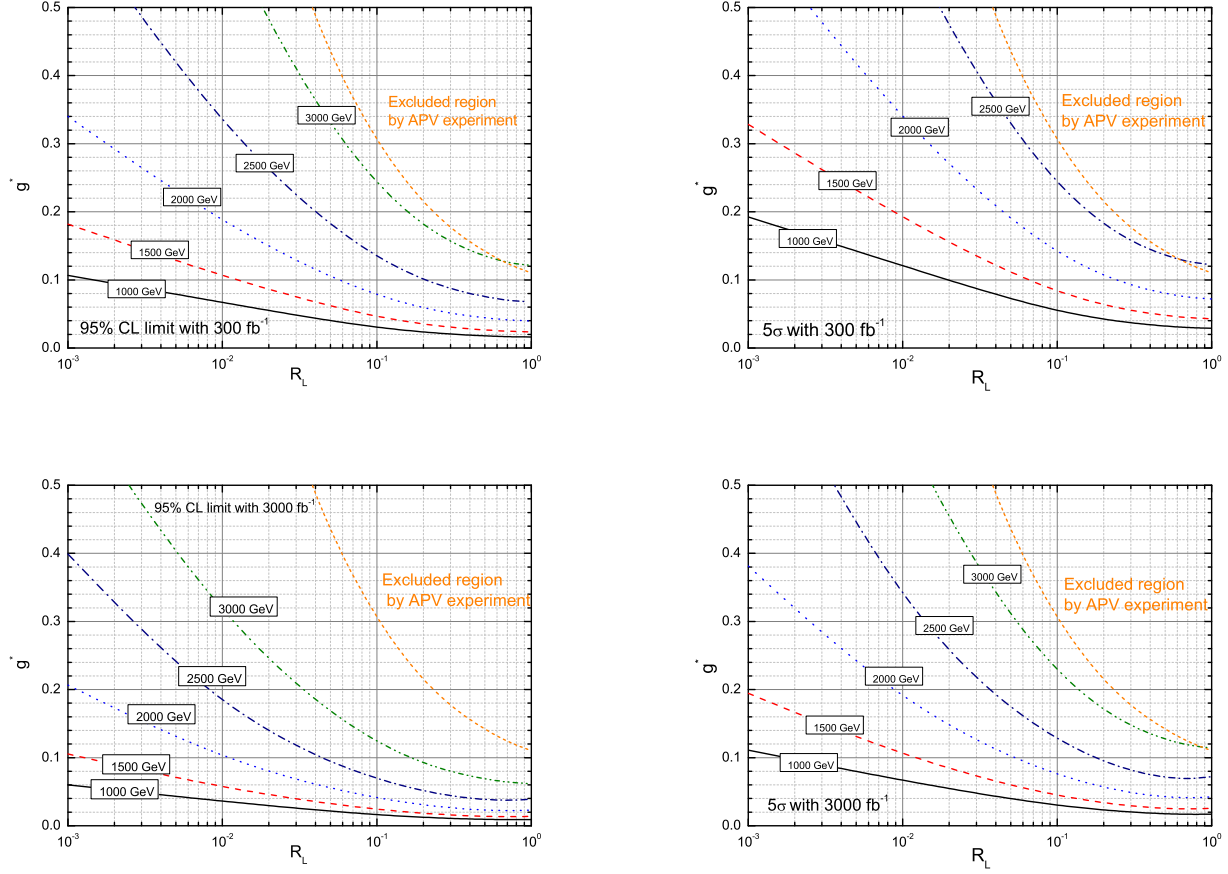


FIG. 7: 95% CL exclusion limit (left panel) and 5σ (right panel) contour plots for the signal in $g^* - R_L$ for five typical mass parameters at 14 TeV LHC with an integrated luminosity of 300 fb^{-1} (upper) and 3000 fb^{-1} (down). Here we take a mild systematic of $\delta = 10\%$.

3000 fb^{-1} . Otherwise, the 95% CL excluded region for the coupling parameter g^* is respectively about 0.05 (0.025), 0.08 (0.04), 0.14 (0.07) with an integrated luminosity of 300 (3000) fb^{-1} .

IV. CONCLUSION

We have present a study of the single production of VLQ- X at the future 14 TeV LHC. The work is performed in a simplified model that the SM extended with an SU(2) doublet $X_{5/3}$ assuming the VLQ- X coupling only to the first- and preferentially to third-generation quarks. We presented a search strategy at the future HL-LHC for a distinguishable signal with a same-sign dilepton plus one b -tagged jet and missing energy. After performing a detector level simulation for the signal and relevant SM backgrounds, the 5σ discovery prospects and 95% CL exclusion limits in the parameter plane were, respectively, obtained at 14 TeV LHC with an integral luminosity of 300 (3000) fb^{-1} , as displayed in Table III. Assuming $Br(X \rightarrow tW) = 1$, the authors in Refs. [88, 89] investigated the expected limits for the VLQ- X via the single production of X at the LHC. Therefore, we also present these results in Table III, where the systematic uncertainty is taken as $\delta = 30\%$ in Ref. [88] and $\delta = 20\%$ in Ref. [89], respectively.

TABLE III: The 95% CL exclusion limits and 5σ signal discoveries at the HL-LHC. The systematic uncertainty is taken as $\delta = 10\%$.

R_L	Luminosity (fb^{-1})	Exclusion		Discovery	
		g^*	$M_X(\text{GeV})$	g^*	$M_X(\text{GeV})$
0	300	[0.12, 0.4]	[1000, 1950]	[0.21, 0.4]	[1000, 1550]
	3000	[0.06, 0.4]	[1000, 2450]	[0.1, 0.4]	[1000, 2000]
0.01	300	[0.07, 0.4]	[1000, 2650]	[0.12, 0.4]	[1000, 2250]
	3000	[0.034, 0.29]	[1000, 3000]	[0.063, 0.4]	[1000, 2700]
0.1	300	[0.027, 0.21]	[1000, 3000]	[0.05, 0.38]	[1000, 3000]
	3000	[0.014, 0.1]	[1000, 3000]	[0.026, 0.2]	[1000, 3000]
1	300	[0.016, 0.12]	[1000, 3000]	[0.003, 0.22]	[1000, 3000]
	3000	[0.008, 0.06]	[1000, 3000]	[0.015, 0.11]	[1000, 3000]
Ref. [88]	300	[0.144, 0.2]	[1000, 1230]	\	\
	3000	[0.082, 0.2]	[1000, 1680]	[0.168, 0.2]	[1000, 1120]
Ref. [89]	3000	[0.12, 0.21]	[1300, 2000]	[0.23, 0.4]	[1300, 2000]

Considering a systematic uncertainty of 10%, the 14 TeV LHC with an integrated luminosity

of 300 fb^{-1} can discover the correlated regions of $g^* \in [0.1, 0.4]$ ($[0.015, 0.22]$) and $M_X \in [1000, 1550]$ $[1000, 3000]$ GeV for $R_L = 0$ (1). On the other hand, the 95% CL exclusion limits are $g^* \in [0.12, 0.4]$ ($[0.01, 0.12]$) and $M_X \in [1000, 1950]$ $[1000, 3000]$ GeV for $R_L = 0$ (1). Meanwhile, the future HL-LHC with an integrated luminosity of 3000 fb^{-1} can discover the correlated regions of $g^* \in [0.1, 0.4]$ ($[0.015, 0.11]$) and $M_X \in [1000, 2000]$ $[1000, 3000]$ GeV for $R_L = 0$ (1). On the other hand, the 95% CL exclusion limits are $g^* \in [0.06, 0.4]$ ($[0.01, 0.06]$) and $M_X \in [1000, 2450]$ $[1000, 3000]$ GeV for $R_L = 0$ (1). We expect that our investigation will represent complementary explorations for a potential VLQ- X at the HL-LHC.

Acknowledgments

This work is supported by the National Natural Science Foundation of China (Grant No. 11904082).

-
- [1] L. Susskind, *Phys. Rev. D* **20**, 2619-2625 (1979).
 - [2] N. Arkani-Hamed, A. G. Cohen, E. Katz, A. E. Nelson, T. Gregoire and J. G. Wacker, *JHEP* **08**, 021 (2002).
 - [3] N. Arkani-Hamed, A. G. Cohen, E. Katz, and A. E. Nelson, *JHEP* **07**, 034 (2002).
 - [4] T. Han, H. E. Logan, B. McElrath and L. T. Wang, *Phys. Rev. D* **67**, 095004 (2003).
 - [5] S. Chang and H. J. He, *Phys. Lett. B* **586**, 95-105 (2004).
 - [6] K. Agashe, R. Contino, and A. Pomarol, *Nucl. Phys. B* **719** 165 (2005).
 - [7] R. Contino, L. Da Rold and A. Pomarol, *Phys. Rev. D* **75**, 055014 (2007).
 - [8] P. Lodone, *JHEP* **12**, 029 (2008).
 - [9] O. Matsedonskyi, G. Panico and A. Wulzer, *JHEP* **01**, 164 (2013).
 - [10] H. J. He, T. M. P. Tait and C. P. Yuan, *Phys. Rev. D* **62**, 011702(R) (2000).
 - [11] X. F. Wang, C. Du and H. J. He, *Phys. Lett. B* **723**, 314-323 (2013).
 - [12] H. J. He, C. T. Hill and T. M. P. Tait, *Phys. Rev. D* **65**, 055006 (2002).
 - [13] H. J. He and Z. Z. Xianyu, *JCAP* **10**, 019 (2014).
 - [14] M. L. Xiao and J. H. Yu, *Phys. Rev. D* **90**, 014007 (2014).
 - [15] K. Agashe, R. Contino, L. Da Rold and A. Pomarol, *Phys. Lett. B* **641**, 62-66 (2006).

- [16] R. S. Chivukula, R. Foadi and E. H. Simmons, *Phys. Rev. D* **84**, 035026 (2011).
- [17] M. Buchkremer, G. Cacciapaglia, A. Deandrea, and L. Panizzi, *Nucl. Phys. B* **876**, 376-417 (2013).
- [18] J. A. Aguilar-Saavedra, R. Benbrik, S. Heinemeyer, and M. Pérez-Victoria,, *Phys. Rev. D* **88**, 094010 (2013).
- [19] J. A. Aguilar-Saavedra, *JHEP* **11**, 030 (2009).
- [20] J. Mrazek and A. Wulzer, *Phys. Rev. D* **81**, 075006 (2010).
- [21] G. Dissertori, E. Furlan, F. Moortgat and P. Nef, *JHEP* **09**, 019 (2010).
- [22] A. Atre, G. Azuelos, M. Carena, T. Han, E. Ozcan, J. Santiago and G. Unel, *JHEP* **08**, 080 (2011).
- [23] G. Cacciapaglia, A. Deandrea, L. Panizzi, N. Gaur, D. Harada and Y. Okada, *JHEP* **03**, 070 (2012).
- [24] G. Cacciapaglia, A. Deandrea, L. Panizzi, S. Perries and V. Sordini, *JHEP* **03**, 004 (2013).
- [25] A. De Simone, O. Matsedonskyi, R. Rattazzi and A. Wulzer, *JHEP* **04**, 004 (2013).
- [26] N. Vignaroli, *JHEP* **07**, 158 (2012).
- [27] S. Gopalakrishna, T. Mandal, S. Mitra and G. Moreau, *JHEP* **08**, 079 (2014).
- [28] O. Matsedonskyi, G. Panico and A. Wulzer, *JHEP* **12**, 097 (2014).
- [29] M. Backović, T. Flacke, S. J. Lee and G. Perez, *JHEP* **09**, 022 (2015).
- [30] C. H. Chen and T. Nomura, *Phys. Rev. D* **94**, 035001 (2016).
- [31] B. Fuks and H. S. Shao, *Eur. Phys. J. C* **77**, 135 (2017).
- [32] K. P. Xie, G. Cacciapaglia and T. Flacke, *JHEP* **10**, 134 (2019).
- [33] J. A. Aguilar-Saavedra, J. Alonso-González, L. Merlo and J. M. No, *Phys. Rev. D* **101**, 035015 (2020).
- [34] A. Belyaev, R. S. Chivukula, B. Fuks, E. H. Simmons and X. Wang, *Phys. Rev. D* **104**, 095024 (2021).
- [35] A. Bhardwaj, T. Mandal, S. Mitra and C. Neeraj, *Phys. Rev. D* **106**, 095014 (2022).
- [36] A. Bhardwaj, K. Bhide, T. Mandal, S. Mitra and C. Neeraj, *Phys. Rev. D* **106**, 075024 (2022).
- [37] S. Verma, S. Biswas, A. Chatterjee and J. Ganguly, *Phys. Rev. D* **107**, 115024 (2023).
- [38] J. Bardhan, T. Mandal, S. Mitra and C. Neeraj, *Phys. Rev. D* **107**, 115001 (2023) .
- [39] J. Z. Han, Y. B. Liu, L. Xing and S. Xu, *Chin. Phys. C* **46**, no.10, 103103 (2022).
- [40] R. Calabrese, A. O. M. Iorio, S. Morisi, G. Ricciardi and N. Vignaroli,

- [Phys. Rev. D **109**, 055030 \(2024\)](#).
- [41] J. M. Alves, G. C. Branco, A. L. Cherchiglia, C. C. Nishi, J. T. Penedo, P. M. F. Pereira, M. N. Rebelo and J. I. Silva-Marcos, [Phys. Rept. **1057**, 1-69 \(2024\)](#).
- [42] A. C. Canbay and O. Cakir, [Phys. Rev. D **108**, 095006 \(2023\)](#).
- [43] A. Belyaev, R. S. Chivukula, B. Fuks, E. H. Simmons and X. Wang, [Phys. Rev. D **108**, 3 \(2023\)](#).
- [44] L. Shang, Y. Yan, S. Moretti and B. Yang, [Phys. Rev. D **109**, no.11, 115016 \(2024\)](#).
- [45] A. Arhrib, R. Benbrik, M. Boukidi, B. Manaut and S. Moretti, [[arXiv:2401.16219 \[hep-ph\]](#)].
- [46] A. Arhrib, R. Benbrik, M. Boukidi and S. Moretti, [[arXiv:2403.13021 \[hep-ph\]](#)].
- [47] B. Yang, Z. Li, X. Jia, S. Moretti and L. Shang, [[arXiv:2405.13452 \[hep-ph\]](#)].
- [48] A. Arhrib, R. Benbrik, M. Berrouj, M. Boukidi and B. Manaut, [[arXiv:2407.01348 \[hep-ph\]](#)].
- [49] Yan-Ju Zhang, Jin-Long Chang, Tai-Gang Liu, [Chin. Phys. C **48**, 073104 \(2024\)](#).
- [50] M. Aaboud *et al.* [ATLAS], [JHEP **08**, 048 \(2018\)](#).
- [51] M. Aaboud *et al.* [ATLAS], [JHEP **12**, 039 \(2018\)](#).
- [52] M. Aaboud *et al.* (ATLAS Collaboration), [Phys. Rev. Lett. **121**, 211801 \(2018\)](#).
- [53] S. Chatrchyan *et al.* [CMS], [Phys. Rev. Lett. **112**, 171801 \(2014\)](#).
- [54] A. M. Sirunyan *et al.* [CMS], [JHEP **08**, 073 \(2017\)](#).
- [55] A. M. Sirunyan *et al.* (CMS Collaboration), [Phys. Rev. D **100**, 072001 \(2019\)](#).
- [56] A. Buckley, J. M. Butterworth, L. Corpe, D. Huang, and P. Sun, [SciPost Phys. **9**, 069 \(2020\)](#).
- [57] A. M. Sirunyan *et al.* [CMS], [JHEP **03**, 082 \(2019\)](#).
- [58] G. Aad *et al.* [ATLAS], [Eur. Phys. J. C **83**, 719 \(2023\)](#).
- [59] S. Moretti, D. O'Brien, L. Panizzi, and H. Prager, [Phys. Rev. D **96**, 075035 \(2017\)](#).
- [60] A. Carvalho, S. Moretti, D. O'Brien, L. Panizzi, and H. Prager, [Phys. Rev. D **98**, 015029 \(2018\)](#).
- [61] A. Deandrea, T. Flacke, B. Fuks, L. Panizzi, and H. S. Shao, [JHEP **08**, 107 \(2021\)](#).
- [62] A. M. Sirunyan *et al.* [CMS], [Eur. Phys. J. C **79**, 90 \(2019\)](#).
- [63] G. Apollinari, O. Brüning, T. Nakamoto and L. Rossi, [CERN Yellow Rep., 1-19 \(2015\)](#).
- [64] R. Contino and G. Servant, [JHEP **06**, 026 \(2008\)](#).
- [65] J. Ren, R. Q. Xiao, M. Zhou, Y. Fang, H. J. He and W. Yao, [JHEP **06**, 090 \(2018\)](#).
- [66] H. Zhou and N. Liu, [Commun. Theor. Phys. **72**, 105201 \(2020\)](#).
- [67] H. Zhou and N. Liu, [Phys. Rev. D **101**, 115028 \(2020\)](#).
- [68] C. W. Chiang, S. Jana and D. Sengupta, [Phys. Rev. D **105**, 5 \(2022\)](#).

- [69] F. X. Yang, Z. L. Han and Y. Jin, *Chin. Phys. C* **45**, 073114 (2021).
- [70] X. M. Cui, Y. Q. Li and Y. B. Liu, *Phys. Rev. D* **106**, 115025 (2022).
- [71] E. Arganda, L. Da Rold, A. Juste, A. D. Medina and R. M. Sandá Seoane, *JHEP* **01**, 156 (2024).
- [72] S. Chatrchyan *et al.* [CMS], *JHEP* **01**, 154 (2013).
- [73] [ATLAS], *ATLAS-CONF-2012-130*.
- [74] F. del Aguila, M. Perez-Victoria and J. Santiago, *JHEP* **09**, 011 (2000).
- [75] R. Mehdiev, A. Siodmok, S. Sultansoy and G. Unel, *Eur. Phys. J. C* **54**, 507-516 (2008).
- [76] F. del Aguila, J. A. Aguilar-Saavedra, B. C. Allanach, J. Alwall, Y. Andreev, D. Aristizabal Sierra, A. Bartl, M. Beccaria, S. Bejar and L. Benucci, *et al.* *Eur. Phys. J. C* **57**, 183-308 (2008).
- [77] A. Atre, M. Carena, T. Han and J. Santiago, *Phys. Rev. D* **79**, 054018 (2009).
- [78] G. Cacciapaglia, A. Deandrea, D. Harada and Y. Okada, *JHEP* **11**, 159 (2010).
- [79] N. Vignaroli, *Phys. Rev. D* **86**, 115011 (2012).
- [80] N. Bonne and G. Moreau, *Phys. Lett. B* **717**, 409-419 (2012).
- [81] J. A. Aguilar-Saavedra, *EPJ Web Conf.* **60**, 16012 (2013).
- [82] K. Ishiwata, Z. Ligeti and M. B. Wise, *JHEP* **10**, 027 (2015).
- [83] H. J. He, N. Polonsky and S. f. Su, *Phys. Rev. D* **64**, 053004 (2001).
- [84] S. Beauceron, G. Cacciapaglia, A. Deandrea and J. D. Ruiz-Alvarez, *Phys. Rev. D* **90**, 115008 (2014).
- [85] L. Basso and J. Andrea, *JHEP* **02**, 032 (2015).
- [86] Y. B. Liu, *Phys. Rev. D* **95**, 035013 (2017).
- [87] G. Aad *et al.* [ATLAS], [[arXiv:2405.19862](https://arxiv.org/abs/2405.19862)] [hep-ex].
- [88] L. Shang and K. Sun, *Nucl. Phys. B* **990**, 116185 (2023).
- [89] J. Z. Han, S. Xu, W. J. Mao and H. Q. Song, *Nucl. Phys. B* **992**, 116235 (2023).
- [90] J. Cao, L. Meng, L. Shang, S. Wang and B. Yang, *Phys. Rev. D* **106**, 055042 (2022).
- [91] A. K. Alok, S. Banerjee, D. Kumar, S. U. Sankar and D. London, *Phys. Rev. D* **92**, 013002 (2015).
- [92] G. Cacciapaglia, A. Deandrea, N. Gaur, D. Harada, Y. Okada and L. Panizzi, *JHEP* **09**, 012 (2015).
- [93] D. Vatsyayan and A. Kundu, *Nucl. Phys. B* **960**, 115208 (2020).
- [94] D. Barducci, A. Belyaev, J. Blamey, S. Moretti, L. Panizzi and H. Prager, *JHEP* **07**, 142 (2014).
- [95] J. Alwall, R. Frederix, S. Frixione, V. Hirschi, F. Maltoni, O. Mattelaer, H.-S. Shao, T. Stelzer, P.

- Torrielli, and M. Zaro, *JHEP* **07**, 079 (2014).
- [96] R. D. Ball *et al.* [NNPDF Collaboration], *JHEP* **04**, 040 (2015).
- [97] B. Jager, C. Oleari and D. Zeppenfeld, *Phys. Rev. D* **80**, 034022 (2009).
- [98] T. Melia, K. Melnikov, R. Rontsch and G. Zanderighi, *JHEP* **12**, 053 (2010).
- [99] J. M. Campbell and R. K. Ellis, *JHEP* **07**, 052 (2012).
- [100] M. Czakon, P. Fiedler and A. Mitov, *Phys. Rev. Lett.* **110**, 252004 (2013).
- [101] T. Sjöstrand, S. Ask, J. R. Christiansen *et al.*, *Comput. Phys. Commun.* **191**, 159 (2015).
- [102] J. de Favereau *et al.* (DELPHES 3 Collaboration), *JHEP* **02**, 057 (2014).
- [103] E. Conte, B. Fuks, and G. Serret, *Comput. Phys. Commun.* **184**, 222 (2013).
- [104] E. Conte, B. Dumont, B. Fuks and C. Wymant, *Eur. Phys. J. C* **74**, 3103 (2014).
- [105] G. Cowan, K. Cranmer, E. Gross, and O. Vitells, *Eur. Phys. J. C* **71**, 1554 (2011) [erratum: *Eur. Phys. J. C* **73**, 2501 (2013)].